Non-Steroidal Anti-Inflammatory Drugs Conjugated to a Synthetic Peptide Exhibits *in vitro* Cytotoxic Activity Against Cervical Cancer and Melanoma Cells

Daniel Alejandro Castellar-Almonacid[a], Andrea Carolina Barragán-Cárdenas[b], Karla Geraldine Rodríguez-Mejia[a], Laura Angélica Maldonado-Sanabria[a], Natalia Ardila-Chantré[a], Jose David Mendoza-Mendoza[b], Claudia Marcela Parra-Giraldo[c], Jhon Erick Rivera-Monroy[d], Zuly Jenny Rivera-Monroy[e], Javier Eduardo García-Castañeda[a], and Ricardo Fierro Medina[e]

[a.] *Departamento de Farmacia-Facultad de Ciencias, Universidad Nacional de Colombia-Sede Bogotá, Bogotá. D.C, Colombia*
[b.] *Instituto de Biotecnología-Facultad de Ciencias, Universidad Nacional de Colombia-Sede Bogotá, Bogotá. D.C, Colombia*
[c.] *Biomedical Sciences Faculty- Universidad Europea, Madrid, España*
[d.] *Universidad de la Salle, LIAC, Bogotá. D.C, Colombia*
[e.] *Departamento de Química-Facultad de Ciencias, Universidad Nacional de Colombia-Sede Bogotá, Bogotá. D.C, Colombia*

Supplementary Material

NAP-1: NAP-RWQWRWQWR

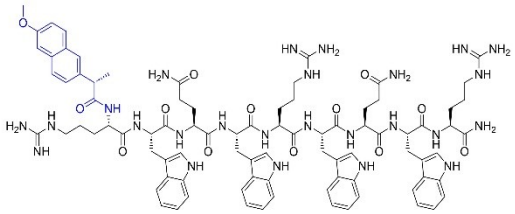

IBU-1: IBU-RWQWRWQWR

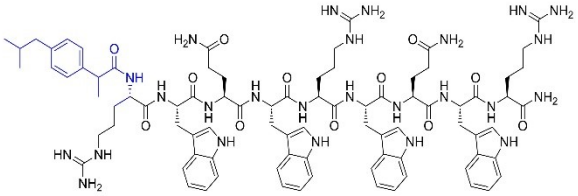

NAP-Orn$_3$1: NAP-OOO-RWQWRWQWR

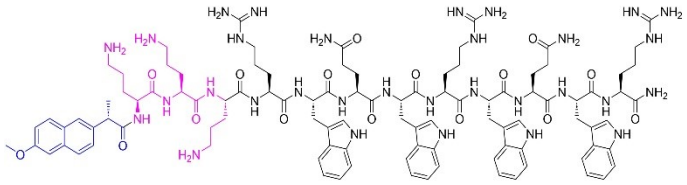

IBU-Orn$_3$-1: IBU-OOO-RWQWRWQWR

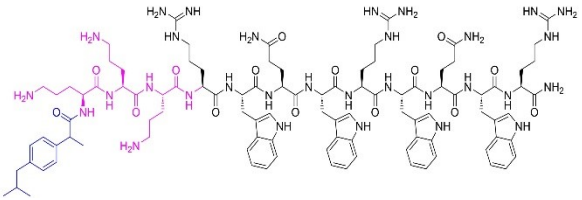

Figure S1. Structures of NSAID-peptide conjugates. The conjugated peptides consist of the palindromic sequence (black) with or without a spacer (three Ornithine residues in pink) and the NSAID (blue) attached at the N-terminal end of the sequence

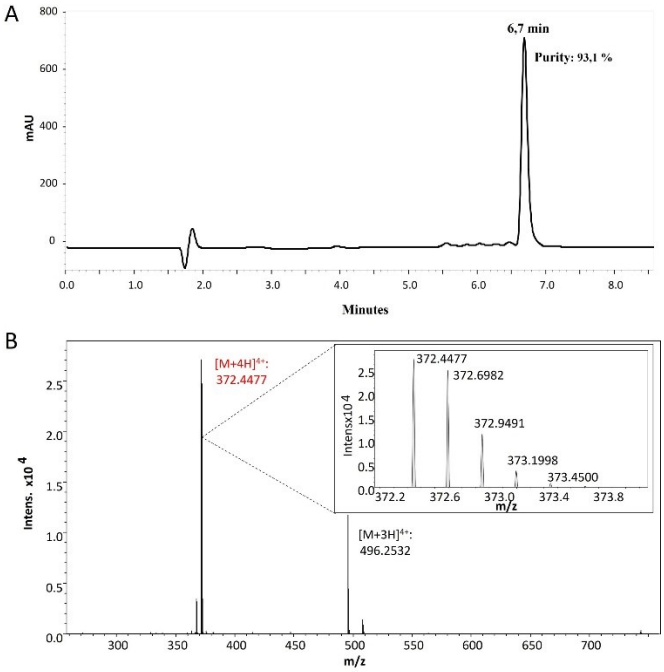

Figure S2. The analytical characterization by RP-HPLC and HRMS ESI-QTOF of the peptide 1: RWQWRWQWR. (A) Chromatographic profile with the retention time and purity percentage displayed. (B) ESI-QTOF mass spectra with the main multiple charged species identified and the isotopic distribution for the base peak.

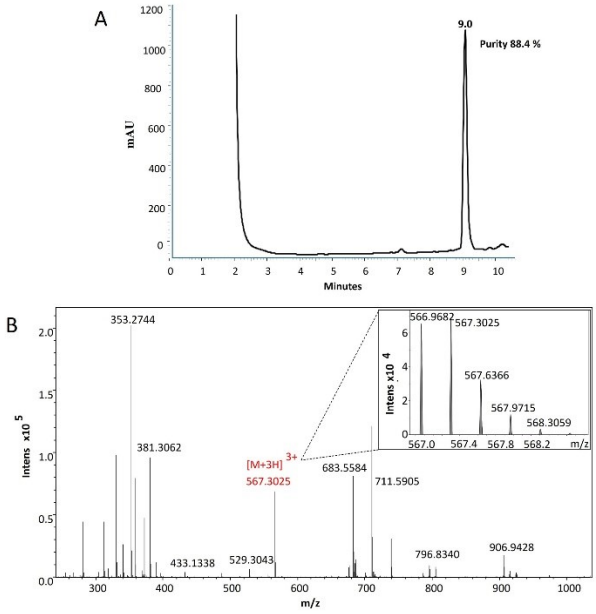

Figure S3. The analytical characterization by RP-HPLC and HRMS ESI-QTOF of the peptide NAP-1: NAP-RWQWRWQWR. (A) Chromatographic profile with the retention time and purity percentage displayed. (B) ESI-QTOF mass spectra with the main multiple charged species identified and the isotopic distribution for the base peak.

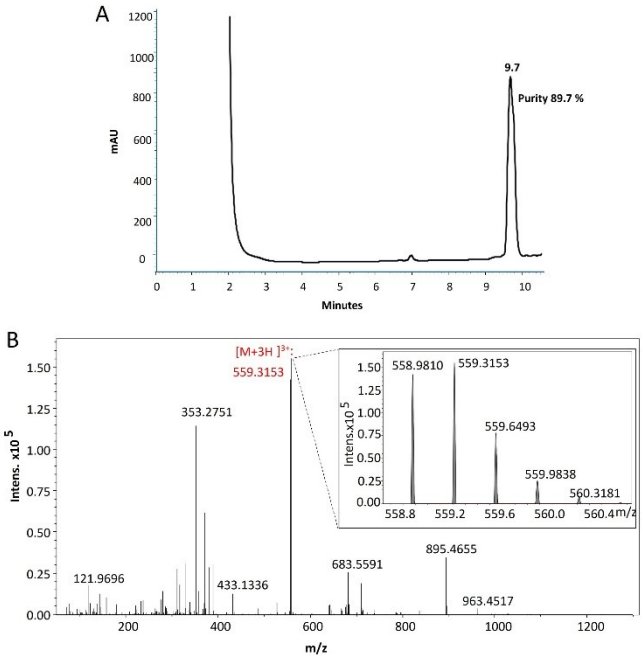

Figure S4. The analytical characterization by RP-HPLC and HRMS ESI-QTOF of the peptide IBU-1: IBU-RWQWRWQWR. (A) Chromatographic profile with the retention time and purity percentage displayed. (B) ESI-QTOF mass spectra with the main multiple charged species identified and the isotopic distribution for the base peak.

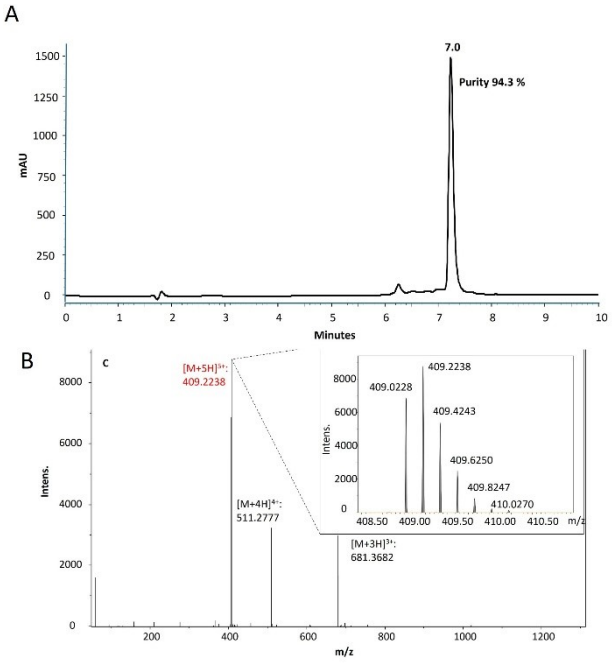

Figure S5. The analytical characterization by RP-HPLC and HRMS ESI-QTOF of the peptide NAP-Orn$_3$-1: NAP-Orn$_3$-RWQWRWQWR (A) Chromatographic profile with the retention time and purity percentage displayed. (B) ESI-QTOF mass spectra with the main multiple charged species identified and the isotopic distribution for the base peak.

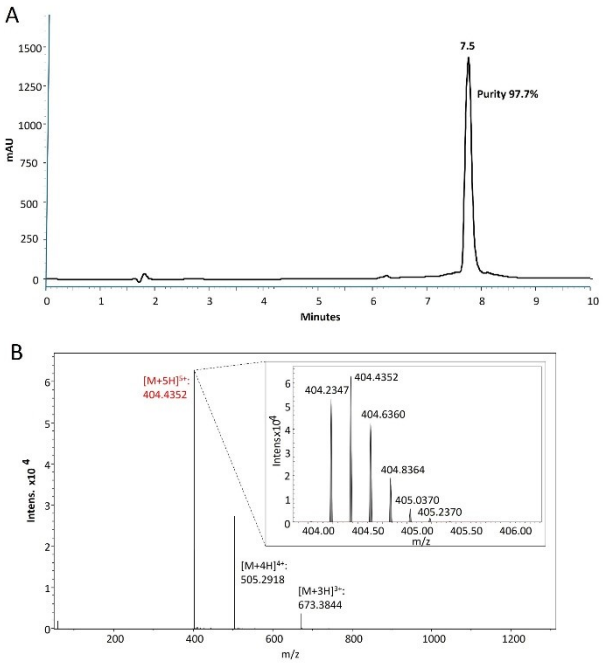

Figure S6. The analytical characterization by RP-HPLC and HRMS ESI-QTOF of the peptide IBU-Orn$_3$-1: IBU-Orn$_3$-RWQWRWQWR (A) Chromatographic profile with the retention time and purity percentage displayed. (B) ESI-QTOF mass spectra with the main multiple charged species identified and the isotopic distribution for the base peak.

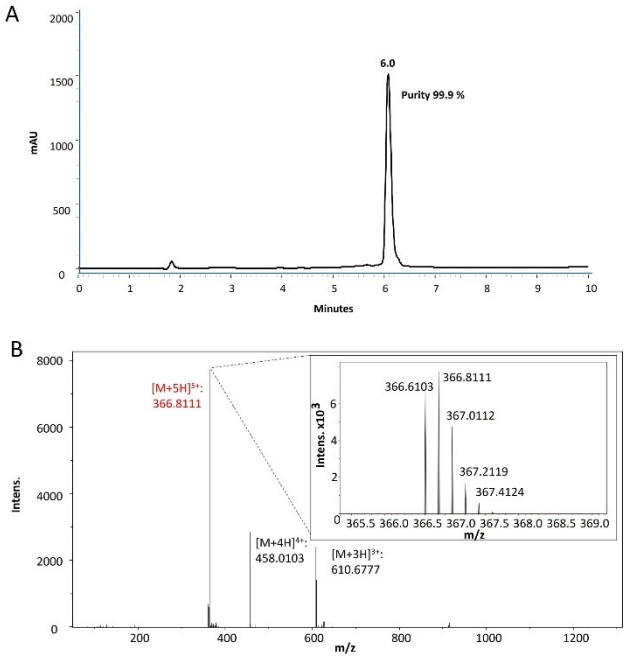

Figure S7. The analytical characterization by RP-HPLC and HRMS ESI-QTOF of the peptide Orn_3-1: Orn_3-RWQWRWQWR (A) Chromatographic profile with the retention time and purity percentage displayed. (B) ESI-QTOF mass spectra with the main multiple charged species identified and the isotopic distribution for the base peak.

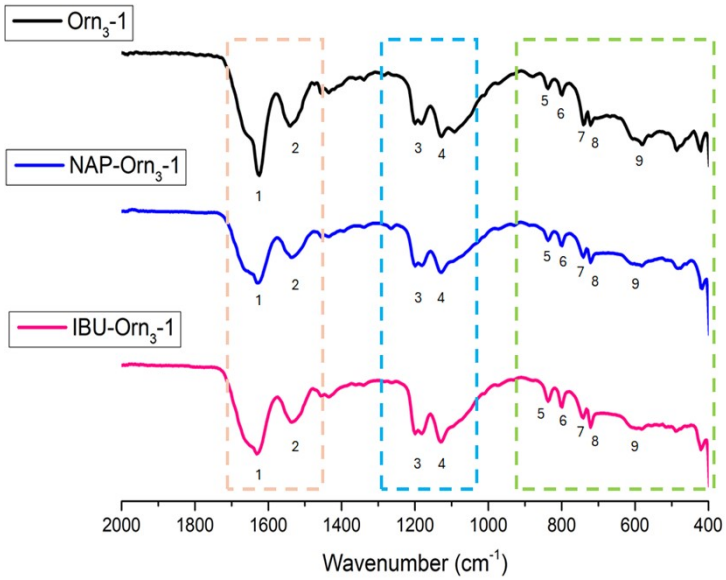

Signal	Group	Wavenumber cm-1
1	Stretching C=O	1655
2	Stretching C=N Bending N-H	1543
3	Stretching C-F (TFA counterion)	1204
4		1134
5	Fingerprint Region	837
6		798
7		740
8		721
9		578

Figure S8. FT-IR ATR spectra of (A) Orn_3-1 (B) NAP-Orn_3-1 (C) IBU-Orn_3-1. FT-ATR spectra were acquired in a Shimadzu IRAffinity1S with a Spec ATR module. Parameters were as follows: Wavelength range 500-4500 cm-1, number of scans 64, Resolution 8.

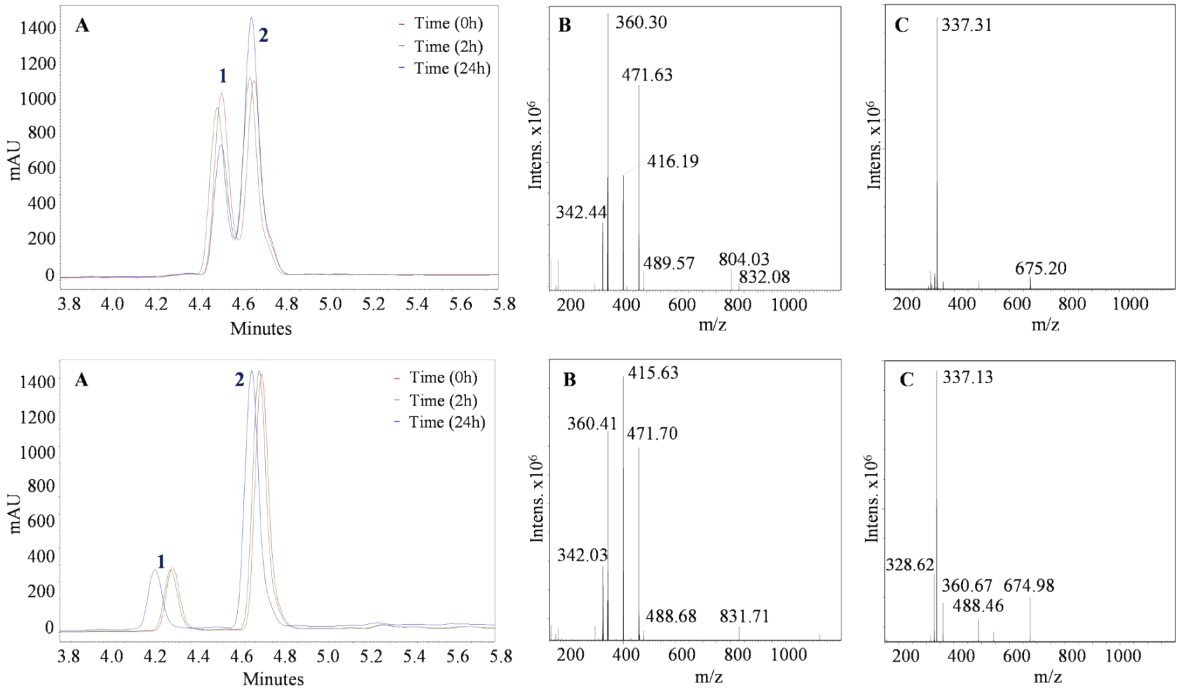

Figure S9. (Top panel) Expanded chromatographic profile of peptide 1 after digestion with trypsin (A) at different time points: 1 min (red), 2 h (green), and 24 h (blue). Mass spectrum of peptide 1: peak 1 (t_R = 4.5 min) is shown in (B), and mass spectrum of peak 2 (t_R = 4.7 min) is shown in (C). (Bottom panel) Expanded chromatographic profile of peptide NAP-Orn_3-1 after digestion with trypsin (A) at different time points: 1 min (red), 2 h (green), and 24 h (blue). Mass spectrum of peptide NAP-Orn_3-1: peak 1 (tR = 4.3 min) is shown in (B), and mass spectrum of peak 2 (tR = 4.7 min) is shown in (C).

Table S1. Peptide fragments identified in the mass spectra of peptides 1 and NAP-Orn_3-1 after trypsin treatment.

m/z experimental	Specie	Fragment	m/z expected
831.70	$[M+H]^+$	RWQWR	831.44
471.70	$[M+H]^+$	RWQ with loss of water	471.24
415.63	$[M+2H]^{2+}$	RWQWR	416.22
360.41	$[M+H]^+$	WR	361.20
342.03	$[M+H]^+$	WR with loss of water	342.18

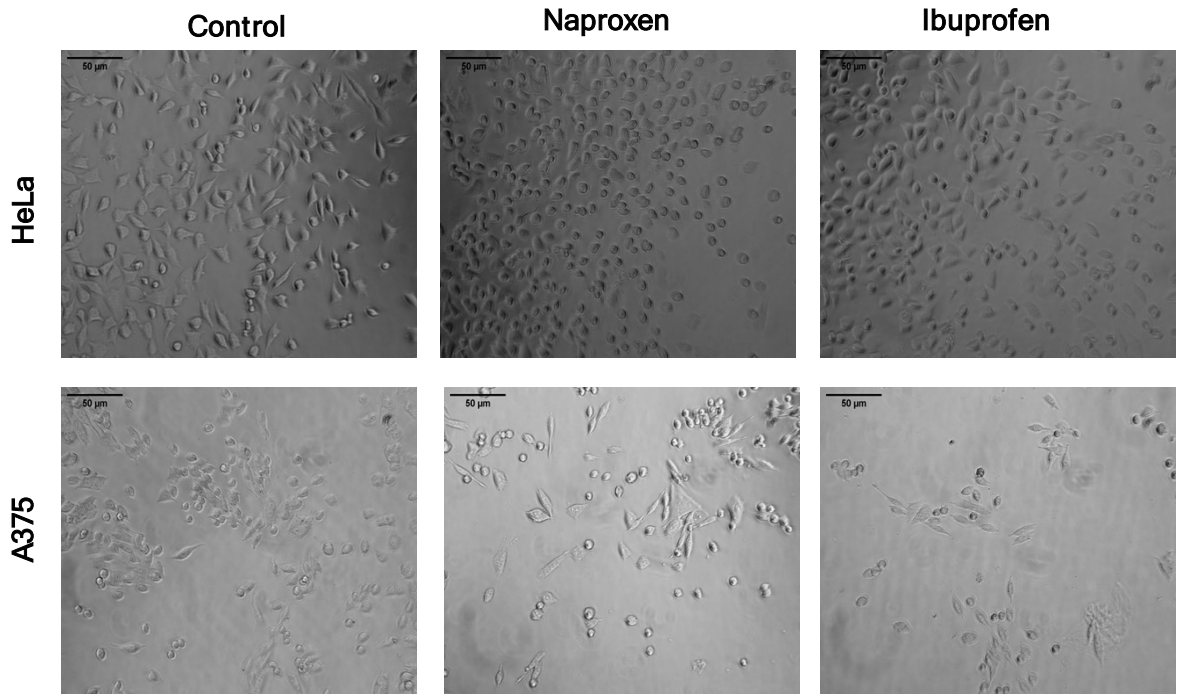

Figure S10. Microphotographs of HeLa and A375 (37ºC) cells after 2h of treatment with 1600 µg/mL of NSAID molecules Naproxen and Ibuprofen.

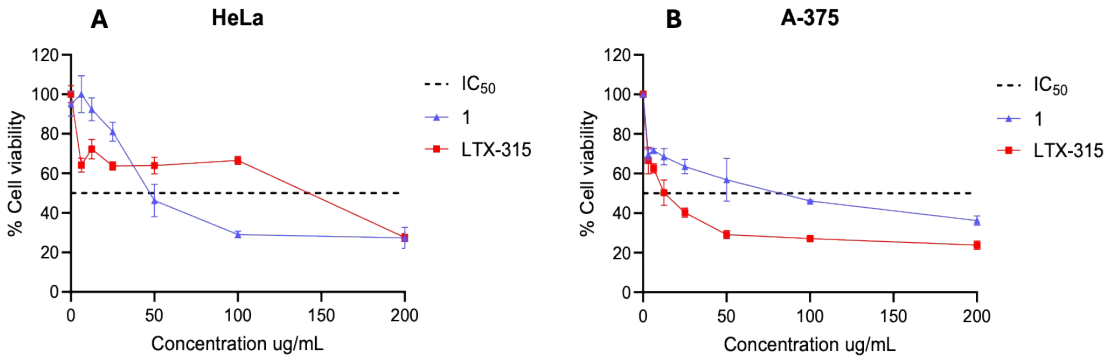

Figure S11. Cell viability plots in cervical cancer (A) and melanoma cells (B) for 1 and LTX-315 (KKWKKW-Dip-K-NH_2). Data represents the mean ± S.D (n=3) (Two-way ANOVA and Sidak´s multiple comparisons tests were performed, p <0.05). Oncolytic peptide LTX-315 was used as a control in the MTT assay. LTX-315 exhibited higher cytotoxicity than peptide 1 in the A-375 cell line, while peptide 1 demonstrated greater activity at concentrations above 50 µg/mL in the HeLa cell line.

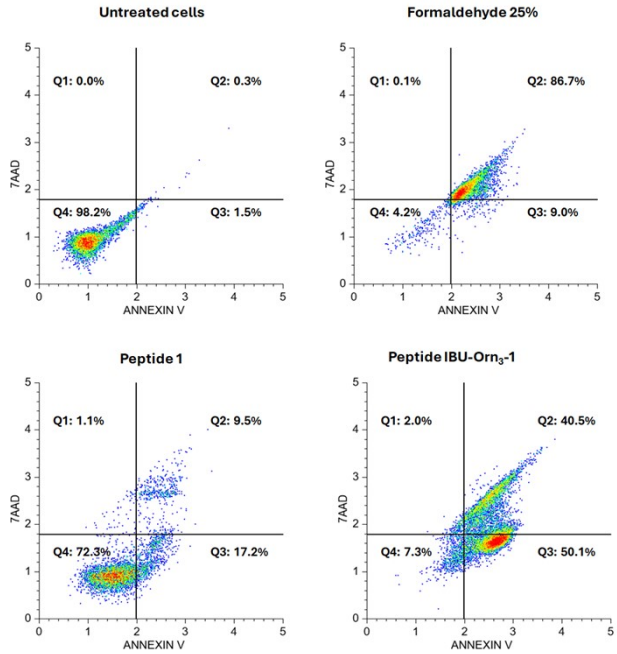

Figure S12. Cytometry assays of the HeLa cells treated with peptides IBU-Orn3-1 (60 µg/mL) or 1 (48 µg/mL) by 24h at 37oC. The plots showed the population's distribution; left upper quadrant Q1: Necrosis; right upper quadrant Q2: later apoptosis; lower right quadrant Q3: early apoptosis, and lower left quadrant Q4: live cells. Negative control: cells untreated; Positive control: Formaldehyde 25%

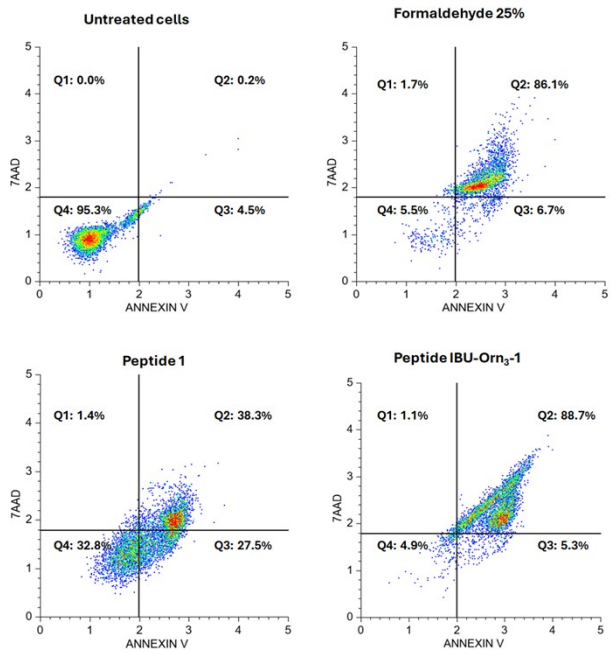

Figure S13. Cytometry assays of the HeLa cells treated with peptides IBU-Orn3-1 (120 µg/mL) or 1 (96 µg/mL) by 2h at 37ºC. The plots showed the population's distribution; left upper quadrant Q1: Necrosis; right upper quadrant Q2: later apoptosis; lower right quadrant Q3: early apoptosis, and lower left quadrant Q4: live cells. Negative control: cells untreated; Positive control: Formaldehyde 25%

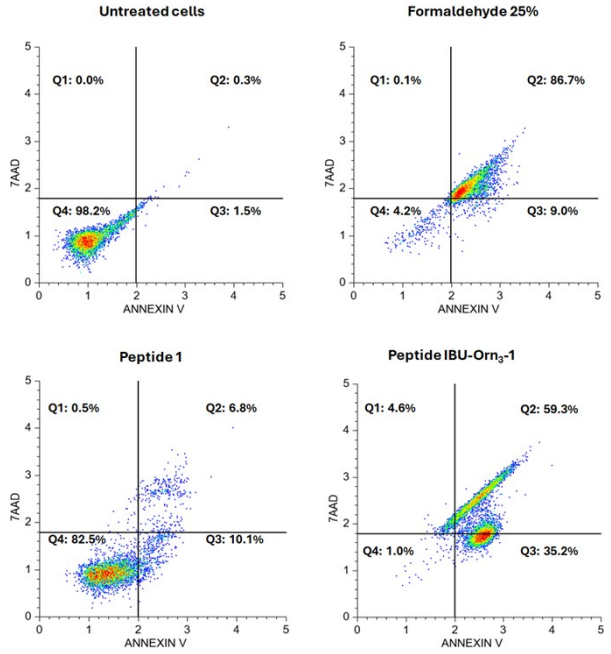

Figure S14. Cytometry assays of the HeLa cells treated with peptides IBU-Orn$_3$-1 (120 µg/mL) or 1 (96 µg/mL) by 24h at 37ºC. The plots showed the population's distribution; left upper quadrant Q1: Necrosis; right upper quadrant Q2: later apoptosis; lower right quadrant Q3: early apoptosis, and lower left quadrant Q4: live cells. Negative control: cells untreated; Positive control: Formaldehyde 25%

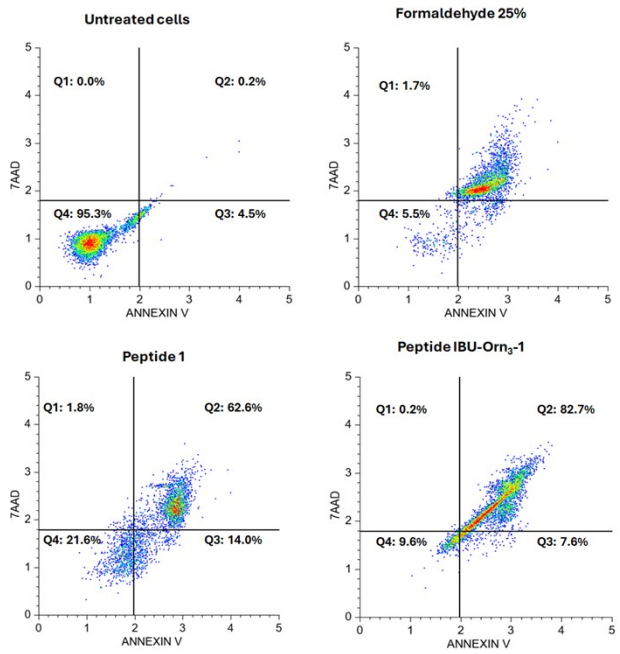

Figure S15. Cytometry assays of the HeLa cells treated with peptides IBU-Orn$_3$-1 (180 µg/mL) or 1 (192 µg/mL) by 2h at 37ºC. The plots showed the population's distribution; left upper quadrant Q1: Necrosis; right upper quadrant Q2: later apoptosis; lower right quadrant Q3: early apoptosis, and lower left quadrant Q4: live cells. Negative control: cells untreated; Positive control: Formaldehyde 25%

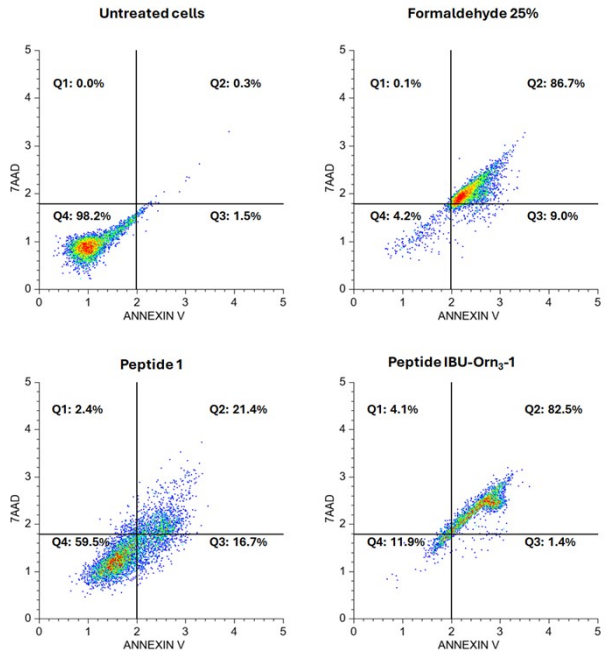

Figure S16. Cytometry assays of the HeLa cells treated with peptides IBU-Orn$_3$-1 (180 µg/mL) or 1 (192 µg/mL) by 24h at 37ºC. The plots showed the population's distribution; left upper quadrant Q1: Necrosis; right upper quadrant Q2: later apoptosis; lower right quadrant Q3: early apoptosis, and lower left quadrant Q4: live cells. Negative control: cells untreated; Positive control: Formaldehyde 25%.

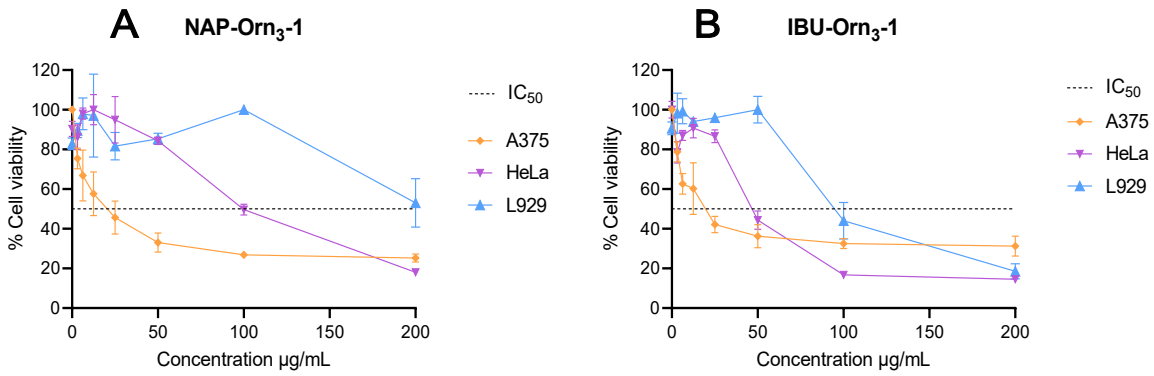

Figure S17. Cell viability plots in Murine Fibroblasts (L929), human cervical cancer (HeLa), and human melanoma (A375) cells for **A)** NAP-Orn)-1 **B)** IBU-Orn_3-1. Data represents the mean+ S.D (n=3) (Two-way ANOVA and Sidak´s multiple comparisons tests were performed, $p < 0.05$). Significant statistical differences between the cytotoxic activity in L929 with HeLa cancer cells were found from 100 to 200 µg/mL for NAP-$(Orn)_3$-1 and 50 to 100 µg/mL for IBU-$(Orn)_3$-1. Significant statistical differences were found for L929 and A375 cells from 6.125 to 200 µg/mL for both peptides NAP-$(Orn)_3$-1 and IBU-$(Orn)_3$-1 excluding the 100 µg/mL concentration.

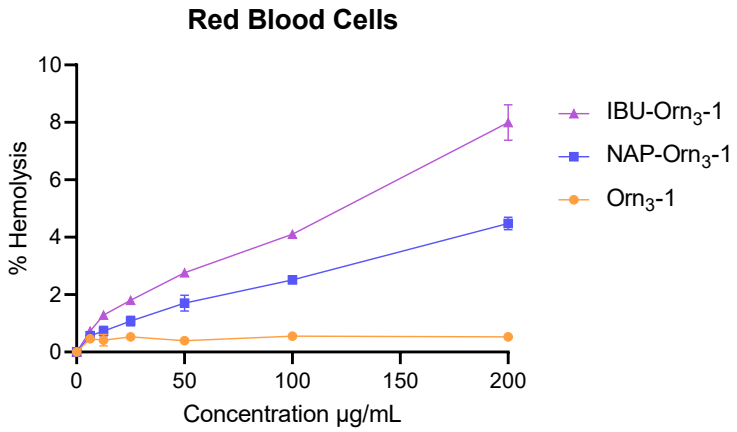

Figure S18. Hemolysis curves for the peptides in the concentration range evaluated (6.25-200 µg/mL)